A variable target intensity-restrained global optimization (VARTIGO) procedure for determining three-dimensional structures of polypeptides from NOESY data: Application to gramicidin-S

Yuan Xu[a], István P. Sugár[b,*] and N. Rama Krishna[a,*]

[a]*Department of Biochemistry and Molecular Genetics, and Comprehensive Cancer Center, The University of Alabama at Birmingham, Birmingham, AL 35294, U.S.A.*
[b]*Departments of Biomathematical Sciences and Physiology and Biophysics, The Mount Sinai Medical Center, New York, NY 10029, U.S.A.*

Summary

A global optimization method for intensity-restrained structure refinement, based on variable target function (VTF) analysis, is illustrated using experimental data on a model peptide, gramicidin-S (GS) dissolved in DMSO. The method (referred to as VARTIGO for *variable target intensity-restrained global optimization*) involves minimization of a target function in which the range of NOE contacts is gradually increased in successive cycles of optimization in dihedral angle space. Several different starting conformations (including all-trans) have been tested to establish the validity of the method. Not all optimizations were successful, but these were readily identifiable from their large NOE R-factors. We also show that it is possible to simultaneously optimize the rotational correlation time along with the dihedral angles. The structural features of GS thus obtained from the successful optimizations are in excellent agreement with the available experimental data. A comparison is made with structures generated from an intensity-restrained single target function (STF) analysis. The results on GS suggest that VARTIGO refinement is capable of yielding better quality structures. Our work also underscores the need for a simultaneous analysis of different NOE R-factors in judging the quality of optimized structures. The NOESY data on GS in DMSO appear to provide evidence for the presence of two orientations for the ornithine side chain, in fast exchange. The NOESY spectra for this case were analyzed using a relaxation rate matrix which is a weighted average of the relaxation rate matrices for the individual conformations.

Introduction

Two-dimensional (2D) nuclear Overhauser enhancement spectroscopy (NOESY) has proved to be a powerful method for the structure elucidation of biological macromolecules (Wüthrich, 1986). The off-diagonal peaks of the NOESY spectra arise from the coupled dipolar relaxation of nuclear spins. Since the dipolar interactions are short range, proton–proton distances in proteins are measurable by NOESY experiments typically only up to ~6 Å. Often, the proton–proton distances are estimated by means of ISPA (isolated spin-pair approximation). Then the method of distance geometry (Crippen and Havel, 1988; Kuntz et al., 1989) is applied to get 3D structures of the

molecule which optimally satisfy the geometric constraints. ISPA is applicable at short mixing times where, unfortunately, the signal-to-noise ratios of the off-diagonal peaks are relatively low. At longer mixing times the signal-to-noise ratio improves, but under these conditions ISPA results in systematic errors in distance estimations (Borgias and James, 1988; Xu and Sugár, 1993) because ISPA neglects the so-called multispin effects, i.e., three-spin effects for small molecules and spin-diffusion effects for large molecules (Krishna et al., 1978).

Structure refinement methods based on total relaxation rate matrix analysis of intensities resolve the above problems (Krishna et al., 1978; Keepers and James, 1984; Borgias and James, 1989). By calculating the complete

---
*To whom correspondence should be addressed.

relaxation rate matrix of the molecule, these methods handle properly the spin-diffusion effects and NOESY spectra can be analyzed at higher mixing times, where the number and intensity of the resolvable off-diagonal peaks are larger. Thus, by using such structure refinement methods, additional and more accurate structural and dynamical information can be extracted from a NOESY spectrum.

Several intensity-restrained structure refinement methods have been proposed that use different optimization strategies (Keepers and James, 1984; Boelens et al., 1988; Borgias and James, 1988,1989,1990; Post et al., 1990). Recently a new method, based on global optimization of a variable target function (VTF), has been developed in our laboratory and carefully tested by using simulated NOESY spectra (Sugár and Xu, 1992; Xu et al., 1994). In this method (referred to as VARTIGO), one optimizes a variable target function involving only NOESY intensities. It thus differs from other VTF-based optimization procedures such as DIANA (Güntert et al., 1991) and DISMAN (Braun and Gō, 1985; Braun, 1987) where the optimization is done on a target function involving interatomic distances and dihedral angles. Recently, Mertz et al. (1991) have implemented an NOE intensity refinement in the VTF algorithm of DIANA. The present paper illustrates the application of the VARTIGO method to the analysis of *experimental* 2D NOESY spectra. To illustrate its application and test its validity, we chose the cyclic decapeptide gramicidin-S (GS), [(L-Val-L-Orn-L-Leu-D-Phe-L-Pro)$_2$], as a suitable system. In addition to being biologically active, it serves as a useful model for antiparallel β-sheet structures in proteins. It has been the subject of several experimental (including NMR) and theoretical investigations. These are quite numerous, and here we will only cite those that are directly pertinent to the current study.

The crystal structure of the hydrated GS–urea complex was determined by Hull et al. (1978). Three years before obtaining the crystal structure, Dygert et al. (1975) computed a minimum energy conformation M1, predicting successfully the backbone structure of the molecule. Several higher energy conformations were also computed by these authors. To test which of these conformations (M1 to M9) was closest to the solution conformation of GS, our laboratory (Huang et al., 1981) carefully measured several 1D NOEs on this peptide and compared them with predicted NOEs for each of the M1–M9 conformations, using a total relaxation rate matrix analysis and NOE R-factors (Krishna et al., 1978). In that study, the rotational correlation time was optimized in a least-squares sense using Marquardt's algorithm to minimize the goodness-of-fit parameter between experimental and calculated NOEs for each of the models, and the corresponding NOE R-factor was calculated (Krishna et al., 1978; Huang et al., 1981). In a global analysis of the

conformations, the three low-energy structures (M1–M3) were found to be equally consistent with the NOE data.

The M1 conformation can be described as a two-stranded antiparallel β-sheet formed by the Val-Orn-Leu sequences, with type II' β-bends at the D-Phe-Pro sequences on both ends. Four backbone hydrogen bonds are formed between the amide protons and carbonyl groups of the valine and leucine residues.

An interesting feature of the M1 conformation is the prediction of a hydrogen bond between the Orn-δNH$_2$ and Phe-CO. Whereas the crystal structure found this hydrogen bond between ornithine and the *following* phenylalanine (i.e., i → i + 2 direction), the M1 structure indicated a bond with the *preceding* phenylalanine (i → i − 3 sense), but with considerable flexibility available for the reorientation of the ornithine side chain. A detailed investigation on GS in methanol by Krauss and Chan (1982) favoured the i → i + 2 bond. The differences between the crystal and the M1 structures have been reconciled by Némethy and Scheraga (1984), who proposed a slightly revised structure (called NS in our notation) that has an ornithine side-chain orientation similar to the crystallographic structure. The χ^1 and χ^2 angles of the ornithine side chain differ significantly between the M1 and NS structures. A [^{1}H-^{13}C]-selective NOE experiment seemed to confirm the presence of such a bond between the Orn-NH$_2$ and Phe-CO groups (Niccolai et al., 1984), although the type of hydrogen bond could not be established. Even though it is not the main focus of the current study, we find NOE evidence for the presence of two types of conformers of GS in DMSO, one with the i → i + 2 and the other with the i → i − 3 hydrogen bond, with approximately equal populations (vide infra).

Several investigators have concentrated on a comparison of proton–proton distances calculated for the M1 structure with those estimated from the NMR studies (e.g., Rae et al., 1977; Jones et al., 1978; Gondol and Van Binst, 1986; Esposito and Pastore, 1988; Mirau, 1988). In this work, we determine the global structure and overall rotational correlation time of the peptide from an analysis of NOESY intensities.

Materials and Methods

NMR spectroscopy

GS hydrochloride was purchased from Sigma Chemical Co. (St. Louis, MO) and used without further purification. The sample was dissolved in deuterated DMSO (Cambridge Isotope Laboratories, Andover, MA) to a concentration of 5 mM. All NMR measurements were performed at 298 K.

^{1}H NMR experiments were carried out on a Bruker AM 600 spectrometer, equipped with an Aspect 3000 computer. NOESY spectra (Macura and Ernst, 1980; Ernst et al., 1986) were recorded at four different mixing

times (75, 100, 150 and 200 ms). 1D NMR, DQF-COSY (Rance et al., 1983) as well as TOCSY (Bax, 1989) experiments were also performed. For the NOESY experiments, 512 t_1 experiments were performed with 2K t_2 complex data points and with a relaxation delay of 1.6 s between scans. The data were processed on a Silicon Graphics workstation using Felix 2.1 software (Biosym Technologies, San Diego, CA). The NOESY data were zero-filled to 1024 points in the t_1 dimension, and the data were double Fourier transformed after multiplying with 2 and 3 Hz exponential window functions in the t_2 and t_1 dimensions, respectively. Fifth-order polynomial baseline corrections were applied after Fourier transformation in the observe dimension. The t_1-ridge suppression was performed using the method of Otting et al. (1986). Volume integrations were performed either automatically or manually, depending on the quality of the peak, with Felix. For each cross peak, the average of the two symmetrically related peaks was calculated and used in intensity-restrained calculations described below.

The variable target intensity-restrained global optimization (VARTIGO) method for structure refinement

In a typical single target function (STF) method, all experimental intensities are optimized *simultaneously*, according to the target function $T(\Omega)$ defined below:

$$T(\Omega) = \sum_{\tau_m} \sum_{(ij)} \left[\frac{\left[A_{ij}^{cal}(\tau_m|\Omega) - A_{ij}^{exp}(\tau_m) \right]^2}{w_{ij}} \right] \quad (1)$$

where $A_{ij}^{exp}(\tau_m)$ is the $(i-j)^{th}$ resolvable integrated peak intensity measured at mixing time τ_m, and w_{ij} ($= \left[|A_{ij}^{exp}| + |A_{ij}^{cal}| \right]^2$) is the respective weight function. The calculated integrated peak intensities A_{ij}^{cal} are given as a function of the Ω vector, where the dihedral angles and the correlation time of the polypeptide are the vector elements. The vector elements of Ω are the optimization parameters.

In the current work, the NOESY spectra of GS have been analyzed by using the intensity-restrained variable target function method (Sugár and Xu, 1992). Recently, this global optimization method was carefully tested by analysis of *simulated* NOESY spectra (Xu et al., 1994). A brief description of the method is given below.

First, we define the range of interacting protons. If a proton from the kth residue of a polypeptide interacts with a proton belonging to the lth residue, then the range of their interaction is $|l-k|$. Then we classify the experimentally available set of resolvable integrated peak intensities {ij}. Let {ij|0} denote the subset of integrated peak intensities (A_{ij}^0) connecting protons i and j, where the range of interacting protons is zero (i.e., in this subset all NOEs are intraresidual). We can define a broader subset {ij|1} of integrated peak intensities (A_{ij}^1) where the range of interacting protons is less than two, and includes the

intraresidue NOE contacts as well as contacts with protons on the nearest-neighbor residues. In general, {ij|k} is a subset of integrated peak intensities A_{ij}^k, where the range of interacting protons is less than $k + 1$. The broadest subset, {ij|$N_r - 1$} = {ij}, contains every resolvable integrated peak intensity, where N_r is the number of residues in the polypeptide. By means of the above classification of the integrated peak intensities we can define the variable target function T_k:

$$T_k(\Omega) = \sum_{\tau_m} \sum_{(ij|k)} \left[\frac{\left[A_{ij}^{k-cal}(\tau_m|\Omega) - A_{ij}^{k-exp}(\tau_m) \right]^2}{w_{ij}} \right] \quad (2)$$

Each A_{ij}^{k-cal} is calculated in two steps. First, by using the *rigid molecule approximation* the relaxation matrix **R** is determined. Then, by means of the semiempirical NOESY theory (Macura and Ernst, 1980) the integrated peak intensities are calculated. In the rigid molecule approximation, the *ij*th element of the relaxation matrix R_{ij} depends on the i–j interproton distance, on the correlation time of the tumbling motion of the molecule and on the Larmor frequencies of the protons (Krishna et al., 1978). For distances involving the protons in a methyl group and an external hydrogen, a simplified $<r^{-3}>$ averaging method (Thomas et al., 1991) was used to take into account the fast internal rotation of methyl groups. An appropriate spectral density function for mutual dipolar relaxation of protons within a methyl group undergoing fast internal rotation was also included (Woessner, 1962). For ring-flip motions (e.g., 2,6 protons of phenylalanine), the $<1/r^6>_{av}$ method was used to account for the slower motions of the aromatic rings (Koning et al., 1990). For more complex motions, specific forms of spectral density functions which are characteristic to the conformation and dynamics of the molecule (Sugár, 1992) may be incorporated into the program.

The optimization now proceeds as follows. The initial values of the parameters of the optimization Ω_0 should define any nonoverlapping polypeptide structure; e.g., an all-trans conformation and reasonable correlation times such as 10 ns for proteins and 1 ns for short polypeptides. By using these initial parameters, one first optimizes the T_0 partial target function in the first iteration, to give the parameter set Ω_1, which in turn provides the initial parameters of the next optimization. In the second optimization cycle, the T_1 partial target function is optimized. The new parameter set Ω_2 obtained from the second optimization provides the initial parameters for the optimization of T_2 in the third cycle. This is followed by the optimization of T_3 in the fourth iteration, and so on. In this way we optimize partial target functions with higher indices in each successive iteration, until in the last cycle the *complete target function* T ($= T_{N_r-1}$) is optimized. For gramicidin-S, we used nine cycles.

The optimization of each partial target function is performed using SUMSNO, a Fortran program which uses numerical gradients and Hessians (Dennis et al., 1981). The VARTIGO algorithm does not involve a backcalculation of the relaxation rate matrix from experimental NOESY intensities. Instead, starting from an initial conformation, the algorithm varies the conformation in increments in dihedral angle space. At each stage, it calculates the relaxation rate matrix and the corresponding predicted NOESY spectra for all mixing times for the intermediate structure, and compares it with the experimental spectra to minimize the target function (Eq. 2). In this method, atomic overlaps are automatically avoided and it is not necessary to explicitly include a separate penalty term in the target function to avoid them. This is because the elements of the relaxation rate matrix increase very fast when atoms approach too close during optimization (Sugár and Xu, 1992).

By using the above optimization strategy one can avoid the local minima of the complete target function T if the number and quality of the constraints are sufficient (Braun and Gō, 1985; Güntert et al., 1991; Sugár and Xu, 1992; Xu et al., 1994). The final polypeptide structure is found through a series of structures satisfying the constraints of the integrated peak intensities, proceeding from shorter to longer range; i.e., during the optimization process the short-range order forms first, followed by formation of the longer range order of the polypeptide structure. This is the essence of the VARTIGO method.

The single target function (STF) approach attempts to optimize *directly* the *complete* target function T (Eq. 1); i.e., it optimizes the NOESY contacts for all ranges simultaneously. Thus, the approach runs a greater risk of missing the global minimum, and may be trapped in some local minimum due to an inefficient conformational search.

All VARTIGO calculations were performed using ECEPP/3 geometrical parameters (Quantum Chemistry Program Exchange, Indiana University, Bloomington, IN) on a CRAY X-MP/216 mainframe computer. Backcalculation of NOESY spectra was done on a Silicon Graphics Iris Indigo workstation using SAS/GRAPH software (SAS Institute, Inc., Cary, NC).

NMR peak assignments

The NMR assignments deduced from TOCSY, NOESY and DQF-COSY spectra were consistent with the published assignments (Jones et al., 1978). The cyclic peptide exhibited the well-known apparent twofold symmetry on the chemical shift scale. Because of this twofold symmetry and the associated chemical shift degeneracy, all peaks in the 2D NOESY spectrum could, in principle, have two alternate assignments (i.e., each cross peak could correspond to protons from either residues i and j or residues i and j + 5). Similar ambiguity occurs in the assignment of resonances from symmetric protein dimers (Nilges, 1993, and references cited therein). Since the purpose of this investigation is to illustrate the VARTIGO refinement procedure using a model peptide, we picked the proper assignments simply from an inspection of the target structure M1. In practically all cases, the proper choice could be made unambiguously because the distances for the two alternate assignments were sufficiently different. In principle, a proper choice of assignments could also be made using NOE R-factor analysis, provided the number of such assignments to be made is rather small. To illustrate this point, we chose two cross peaks (Orn-αH-Leu-NH and Orn-NH-Orn-αH) and computed the R-factors corresponding to the four possible assignments. These are shown in Table 1. It is clear that the combination of Orn^2-αH-Leu^3-NH and Orn^2-NH-Orn^2-αH gives the lowest R_1, R_2 and R_4 values. However, since the number of alternate assignment combinations in GS goes up as 2^n, where n is the number of cross peaks that need to be assigned, such an R-factor analysis becomes prohibitive for n larger than 4.

Scaling of the calculated intensities

Every integrated peak intensity of a NOESY spectrum is directly proportional to the equilibrium magnetization of the molecule, M_0. For fitting of the experimental and calculated NOESY spectra, M_0 can either be considered as one of the optimization parameters or it can be determined before the global optimization. The second option is based on the fact that at zero mixing time, the integrated peak intensities are (Macura and Ernst, 1980):

TABLE 1

COMPARISON OF R-FACTORS[a] FOR FOUR COMBINATIONS OF ASSIGNMENTS FOR TWO CROSS PEAKS (Orn-αH-Leu-NH AND Orn-NH- Orn-αH)[b] IN THE NOESY SPECTRUM OF GRAMICIDIN-S

Assignment	R_m	R_1	R_2	R_4
Orn^2-αH-Leu^8-NH / Orn^2-NH-Orn^7-αH	0.496 (0.33)	0.48 (0.34)	0.4 (0.3)	0.11 (0.07)
Orn^2-αH-Leu^8-NH / Orn^2-NH-Orn^2-αH	0.48 (0.343)	0.478 (0.388)	0.397 (0.331)	0.106 (0.069)
Orn^2-αH-Leu^3-NH / Orn^2-NH-Orn^7-αH	0.487 (0.336)	0.373 (0.368)	0.368 (0.297)	0.11 (0.074)
Orn^2-αH-Leu^3-NH / Orn^2-NH-Orn^2-αH	0.47 (0.33)	0.37 (0.29)	0.36 (0.27)	0.1 (0.066)

[a] The starting values of the R-factors using the M1 structure are given along with VARTIGO-refined values in parentheses.

[b] All other assignments correspond to those expected for the target structure M1.

$$A_{ij}(0) = \left(\frac{M_0}{N_p}\right) n_i \delta_{ij} \qquad (3)$$

where N_p is the number of hydrogen atoms in the molecule and n_i is the number of protons in the ith set of magnetically equivalent hydrogen atoms of the molecule. In order to obtain the equilibrium magnetization M_0, we determined the integrated intensities of diagonal peaks at zero mixing time, $A_{ii}(0)$, by extrapolating resolvable diagonal peaks measured at nonzero mixing times. An extrapolation was performed by fitting the diagonal peak intensities at short mixing times to the sum of two exponentials. The extrapolated values for different single-proton peaks were essentially identical, differing from the average by about 10%. The average M_0 value was used in computation of the NOESY spectra.

Determination of GS conformations from NOESY intensities by VARTIGO refinement

Because of the C_2 symmetry of GS, every resolvable off-diagonal peak belongs to two symmetric proton–proton contacts. From our NOESY spectra 61 resolvable off-diagonal peaks were obtained, resulting in a total of 122 (= 2×61) intensity constraints. Of these, 66 were intraresidual, 38 were (i,i + 1)-type interresidual, four were (i,i + 2) type, while the rest (14) were higher order interresidual constraints. Four of the 18 higher order constraints are between residues 1 and 10 and belong to the (i,i + 1) type if GS were treated as a closed ring. In our calculations, however, GS was treated as a linear decapeptide because in the ECEPP/3 software there is no option for constructing a cyclic polypeptide with the two ends covalently bonded. The NH of Val[1] and the CO of Pro[10] were specified as end groups. Note that during structure refinement, the head and tail of this linear decapeptide were forced by the NOESY constraints to approach each other, eventually forming a ring structure. Obviously, by linearizing the cyclic GS molecule we lost an important, built-in constraint, but the number of intensity constraints was still large enough for successful optimizations. Nevertheless, it is heartening that the NOESY constraints correctly form the ring closure in our calculations (vide infra).

In our previous study on GS, we have optimized the rotational correlation time τ_c to get the best fit between experimental NOEs in GS and NOEs calculated for different models (with fixed dihedral angles), and a value of 1.1 ns was obtained for the best structures (Huang et al., 1981). In the current study, we first did a *simultaneous* optimization of dihedral angles and τ_c for the M1 initial structure, and obtained a value of 0.9 ns. For the rest of the optimizations, we fixed the correlation time at 0.9 ns, primarily because small variations in dihedral angles produce much more pronounced changes in the calculated NOEs than small variations in τ_c.

The partial target functions to be optimized were constructed from the above experimental constraints (NOESY intensities). Each constraint was determined at four mixing times (75, 100, 150 and 200 ms). Optimizations of the target functions were performed by using the VTF method (Eq. 1). Optimizations were run using 18 different starting conformations of GS: all-trans, a minimum-energy structure (called NS in this work) published by Némethy and Scheraga (1984), nine minimum-energy structures (M1 to M9) determined by Dygert et al. (1975), the DeSantis and Liquori structure (1971) (called DL in this work), five minimum-energy structures generated from some of the M1 to M9 structures after energy minimization using the ECEPP/3 energy function, and finally, the average structure ('MEAN' in Table 2) obtained from a starting structure defined by the average dihedral angles of the 13 successfully optimized structures (with $R_1 \leq 0.4$). The criterion for successful optimization is defined below. For comparison, we also performed optimizations using the STF (Eq. 1) for each of the 18 structures.

The optimization incorporated a calculation of NOE R-factors originally introduced by our laboratory (Krishna et al., 1978; Huang et al., 1981) as an indicator of the agreement between calculated and experimental NOEs. The magnitudes of these factors were used in judging the success of the VARTIGO refinement of different starting conformations (Xu et al., 1994). Four different NOE R-factors were calculated, according to the following definitions:

$$R_1 = \left[\frac{\sum\limits_{ijm}^{N} \left[A_{ij}^{exp}(\tau_m) - A_{ij}^{cal}(\tau_m|\Omega) \right]^2}{\sum\limits_{ijm}^{N} \left[A_{ij}^{exp}(\tau_m) \right]^2} \right]^{1/2} \qquad (4)$$

$$R_2 = \frac{\sum\limits_{ijm}^{N} \left| \left[A_{ij}^{exp}(\tau_m) - A_{ij}^{cal}(\tau_m|\Omega) \right] \right|}{\sum\limits_{ijm}^{N} \left| A_{ij}^{exp}(\tau_m) \right|} \qquad (5)$$

$$R_m = \frac{1}{N} \sum\limits_{ijm}^{N} \left[\frac{\left| A_{ij}^{exp}(\tau_m) - A_{ij}^{cal}(\tau_m|\Omega) \right|}{\left| A_{ij}^{exp}(\tau_m) \right|} \right] \qquad (6)$$

$$R_d = \left[\frac{\sum\limits_{ijm}^{N} \left| \left| A_{ij}^{exp}(\tau_m) \right|^{-1/6} - \left| A_{ij}^{cal}(\tau_m|\Omega) \right|^{-1/6} \right|}{\sum\limits_{ijm}^{N} \left| A_{ij}^{exp}(\tau_m) \right|^{-1/6}} \right] \qquad (7)$$

where $A_{ij}^{exp}(\tau_m)$ and $A_{ij}^{cal}(\tau_m|\Omega)$ are the experimental and calculated integrated peak intensities, respectively, of the (i − j)th proton pair at mixing time τ_m; the Ω vector contains the optimization parameters, such as dihedral angles and correlation time; N is the number of terms in the

42

summations, and the summations are taken for the resolvable off-diagonal peaks of the experimental NOESY spectra and for every mixing time. R_1 corresponds to the definition originally introduced by our laboratory (Krishna et al., 1978). R_d is more sensitive to weak NOESY contacts (Gonzalez et al., 1991; Thomas et al., 1991) than R_1. In Table 2, the R-factors calculated at the beginning and end of the optimizations are listed.

In an ideal case, i.e., with zero experimental errors, all the R-factors become zero when the calculated spectra fit best to the experimental ones. At nonzero experimental errors, even in the case of the best fit, the R-factor values are positive. We have previously calculated, using simulated NOESY data on model peptides, the upper estimates of the best R-factors as a function of the average experimental error (Xu et al., 1994). For example, at 40% average simulated experimental error the following upper estimates of the best R-factor values were obtained: $R_m < 0.4$, $R_1 < 0.4$, $R_2 < 0.4$ and $R_d < 0.1$ (Xu et al., 1994). In this study, an optimization was considered successful if $R_1 \leq 0.4$.

In this respect it is important to mention that Thomas et al. (1991), while testing the MARDIGRAS distance refinement method, generated distance constraints from a simulated experimental NOESY spectrum of BPTI. The all-atom rms deviation between the DISGEO-generated conformations from the distance constraints and the BPTI target structure was approximately 1.5 Å, while the respective R-factors from a comparison of calculated and simulated experimental NOESY spectra were $R_1 \approx 0.38$, $R_2 \approx 0.34$ and $R_d \approx 0.09$ for a correlation time of 2 ns.

Results and Discussion

GS structures from VARTIGO refinements

The NOESY spectra of GS have been analyzed using the VARTIGO refinement method. Figure 1 shows six of the 18 starting conformations. Since the all-trans conformation has two steric conflicts that involve the hydrogens associated with phenylalanine and leucine side chains, they were relieved by energy minimization of the side chains. We call this the modified all-trans structure. Of

TABLE 2
COMPARISON OF NOE R-FACTORS BEFORE AND AFTER OPTIMIZATION BY STF AND VARTIGO

Starting conformation[a]		R_m	R_1	R_2	R_d	T	Starting conformation[a]		R_m	R_1	R_2	R_d	T
All-trans[b]	I	4.29	2.54	1.50	0.82		M5(EM)	I	1.19	0.80	0.77	0.19	
	S	0.46	0.44	0.41	0.169	2.43		S	0.39	0.41	0.36	0.101	2.56
	V	0.39	0.33	0.31	0.08	1.74		V	0.35	0.30	0.29	0.07	1.43
M1	I	0.47	0.37	0.36	0.10		M6	I	1.04	0.68	0.64	0.21	
	S	0.35	0.31	0.29	0.067	1.82		S	0.39	0.56	0.39	0.094	2.48
	V	0.33	0.29	0.27	0.066	1.43		V	0.34	0.30	0.29	0.07	1.43
M1(EM)	I	0.47	0.38	0.37	0.10		M7	I	0.63	0.61	0.56	0.28	
	S	0.33	0.29	0.27	0.066	1.43		S	0.47	0.48	0.41	0.143	3.32
	V	0.34	0.28	0.27	0.067	1.43		V	0.47	0.48	0.41	0.14	3.32
M2	I	0.52	0.42	0.42	0.11		M8	I	1.62	0.76	0.79	0.26	
	S	0.35	0.30	0.29	0.067	1.43		S	0.74	0.56	0.51	0.232	3.97
	V	0.35	0.30	0.29	0.07	1.43		V	0.45	0.40	0.35	0.077	2.1
M3	I	0.87	0.50	0.49	0.18		M9	I	2.57	1.23	0.97	0.28	
	S	0.40	0.39	0.35	0.078	1.66		S	0.59	0.68	0.54	0.135	2.31
	V	0.38	0.34	0.32	0.08	1.65		V	0.49	0.55	0.39	0.13	2.23
M3(EM)	I	0.92	0.51	0.51	0.22		M9(EM)	I	1.52	0.79	0.79	0.31	
	S	0.47	0.38	0.30	0.090	1.89		S	0.56	0.65	0.52	0.117	2.22
	V	0.37	0.33	0.30	0.08	1.67		V	0.55	0.66	0.52	0.11	2.2
M4	I	1.47	0.80	0.76	0.17		DL	I	0.52	0.44	0.42	0.10	
	S	0.38	0.32	0.30	0.103	1.91		S	0.34	0.29	0.27	0.066	1.43
	V	0.40	0.35	0.33	0.10	2.1		V	0.34	0.28	0.27	0.066	1.43
M4(EM)	I	1.26	0.78	0.74	0.18		NS	I	1.16	0.44	0.46	0.17	
	S	0.40	0.35	0.33	0.102	2.57		S	0.39	0.36	0.32	0.089	1.84
	V	0.34	0.30	0.29	0.07	1.46		V	0.38	0.29	0.29	0.08	1.68
M5	I	1.38	0.77	0.73	0.16		MEAN[c]	I	0.77	0.80	0.54	0.097	
	S	0.39	0.41	0.36	0.101	1.92	(VARTIGO)	S	0.33	0.28	0.27	0.065	1.43
	V	0.36	0.33	0.31	0.07	1.48		V	0.33	0.28	0.27	0.066	1.43

For each conformation, the entries show the initial value (I, top), and the values after STF (S, middle) and VARTIGO (V, bottom) optimization. Also included are the final values for the two optimized target functions (T).
[a] Structures with (EM) refer to energy-minimized (using ECEPP) starting structures. M1 to M9 are from Dygert et al. (1975); NS is the Némethy–Scheraga structure (1984); and DL is the structure by DeSantis and Liquori (1971).
[b] The all-trans structure was modified by energy minimization of the leucine and phenylalanine side chains to relieve steric conflicts with the protons of neighboring residues.
[c] Generated from average torsion angles of 13 structures with $R_1 \leq 0.4$, and minimized against experimental intensities.
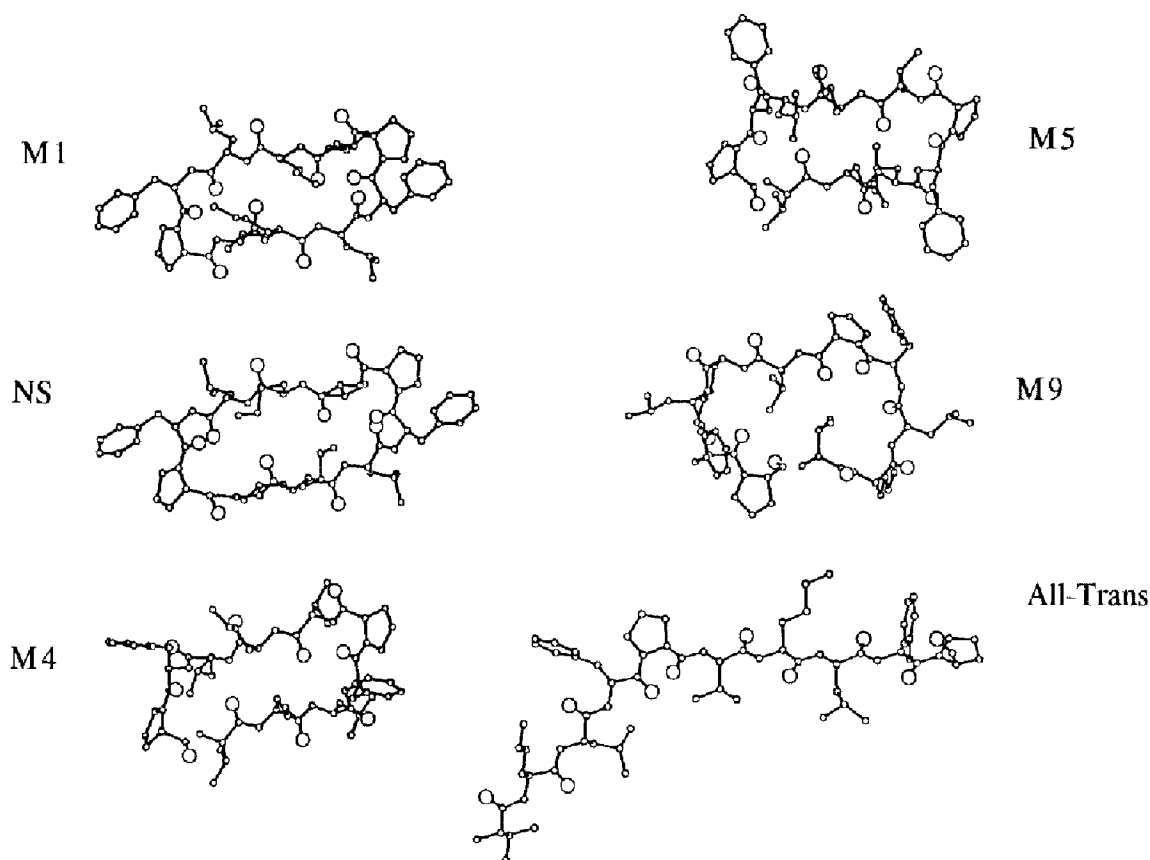
Fig. 1. Six of the 18 starting conformations of gramicidin-S used in NOE intensity-restrained variable target function analysis. The conformations shown are M1, NS, M4, M5, M9 and the modified all-trans structure. Note that the all-trans conformation (bottom right) shows a bend at Pro⁵.

the 18 optimizations, 14 were considered to be successful as judged by R-factors. In Table 2, the R-factors for the 18 structures are listed before and after optimization by STF and VARTIGO procedures. Figure 2 shows a superposition of the 13 VARTIGO-refined structures and their average. The dihedral angles of the VARTIGO MEAN structure are listed in Table 3. The backbone

conformation of GS is well defined in all the optimized structures. The side chain of phenylalanine is relatively poorly defined, since the NMR spectra contained unresolved ring proton resonances for this residue and the phenylalanine further shows fewer nontrivial NOEs compared to other residues.

The average VARTIGO structure of GS shows that it is
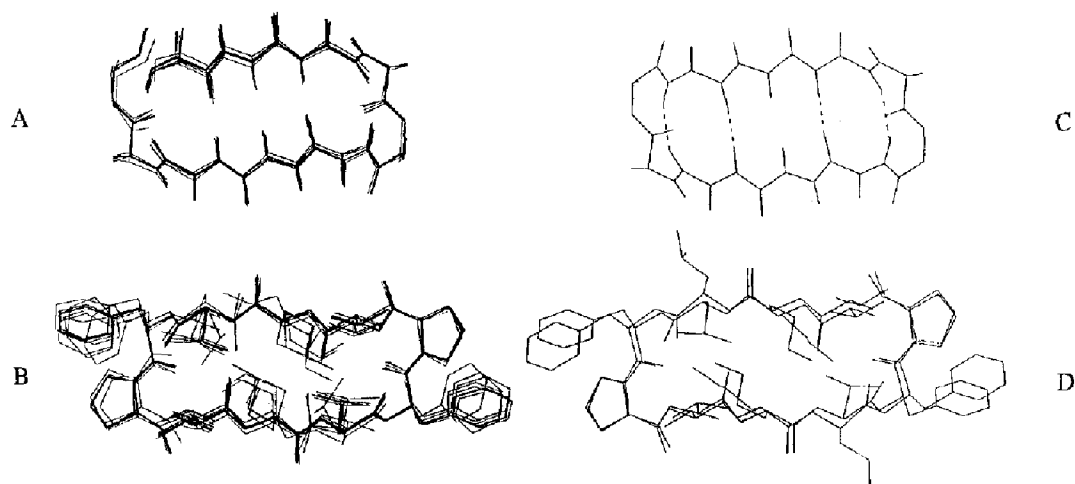
Fig. 2. Superposition of 13 VARTIGO-refined structures. (A) only backbones are shown; (B) both backbones and side chains; (C) the MEAN VARTIGO backbone structure; and (D) superposition of the average VTF and M1 structures.
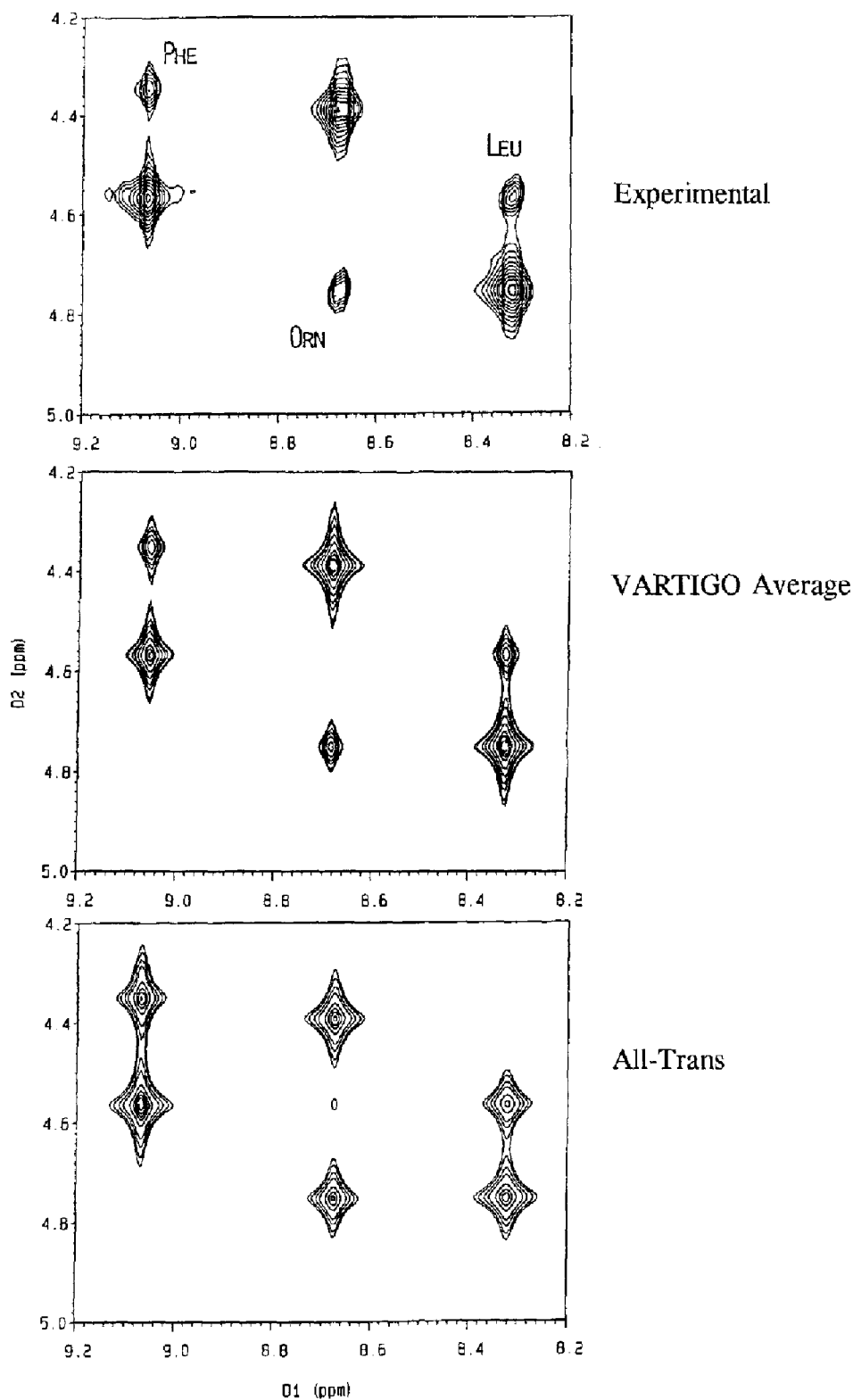
Fig. 3. Comparison of the fingerprint regions of the experimental and backcalculated NOESY spectra for the average VTF structure. Also shown is the spectrum for the modified all-trans conformation.

capable of forming four backbone hydrogen bonds, as well as the ornithine side-chain hydrogen bond with Phe-CO in the i → i − 3 sense as in the M1 structure, even though no explicit hydrogen bond constraints were introduced. In Fig. 2 we show a superposition of the 13 best VTF struc-

tures and the average structure with hydrogen bonds.

In Fig. 3, we show the fingerprint region of the NOESY backcalculated spectrum for the all-trans conformation before and after VARTIGO refinement. Also shown is the corresponding experimental spectrum.

TABLE 3
TORSION ANGLES FOR THE OPTIMIZED AVERAGE VARTIGO STRUCTURE OF GRAMICIDIN-S[a]

Residue	ϕ	ψ	ω	χ^1	χ^2	χ^3	χ^4
Val	−102.07	108.38	180.00	177.87	84.55	29.86	
Orn[b]	−117.92	138.93	180.00	−54.89	−94.93	−174.95	−19.64
Leu	−145.90	78.33	180.00	82.15	108.96	66.07	50.33
D-Phe	70.56	−127.50	180.00	171.68	−80.58		
Pro	−75.00	−8.15	180.00				

[a] The bond lengths and bond angles corresponding to the ring closure of gramicidin-S at residues Val[1] and Pro[10] are: Pro[10] C' - Val[1] N = 1.23 Å, ω = 179.4°, C'(10)-N(1)-Cα(1) = 126.5°, Cα(10)-C'(10)-N(1) = 119.6°, and O(10)-C'(10)-N(1) = 119.9°.

[b] The side-chain torsion angles for ornithine refer to an orientation similar to that in the M1 conformation.

NOE R-factors for VARTIGO refinements

In Table 2, the NOE R-factors are listed for the 18 starting structures before and after optimization. Among the R-factors, R_1 tends to overemphasize the agreement among stronger intensities (shorter distances) because of the r^{-6} dependence, but by the same token it is more sensitive to small differences in shorter distances between structures (e.g., calculated and solution structures). On the other hand, R_d gives a more reasonable weight to larger distances in a given structure, but it is somewhat less sensitive to small variations in distances between different structures. Our experience suggests that it is prudent to examine both types of R-factors in comparing different structures. In addition to these two parameters, we have also calculated the R_2 and R_m factors defined in Eqs. 5 and 6.

An examination of Table 2 shows that *before* optimization, the R_d values ranged from 0.1 to 0.82 (for all-trans). However, *after* VARTIGO optimization, the R_d values were much more reasonable, varying from 0.066 to 0.14. Interestingly, the optimization of the all-trans structure was very successful, with R_d changing from 0.82 to 0.08. The R_1 value for this structure changed from 2.54 before optimization to 0.33 after optimization. Among the 18 structures, R_1 values ≤ 0.4 were obtained for 14 structures. The remaining structures (M7, M9, M9(EM)) had larger R_1 values, indicating that the optimizations were trapped in local minima and unable to approach the global minimum values. Nevertheless, the R_d-factors are not too unreasonable (especially for the M9(EM) structure) for these three bad structures. A visual examination of the optimized M9(EM) structure (not shown) reveals that it is 'twisted' considerably compared to the M1 model. These observations underscore the importance of judging several NOE R-factors in assessing the quality of a calculated structure. An average of the 13 acceptable conformations was calculated and used as a starting conformation for the MEAN (Table 2). The resulting VARTIGO-optimized structure had values of 0.28 for R_1 and 0.066 for R_d. The average rmsd values (with regard to the mean structure) for the backbone atoms of the 14 optimized structures were 0.18 Å for the backbone and 0.72 Å for all heavy atoms.

Comparison between VARTIGO and STF methods

A major concern in many of the NOESY optimization procedures currently in use is the difficulty in finding a global minimum for the conformational search. The variable target function method, however, frequently finds the global minimum, irrespective of the initial conformation (Braun and Gō, 1985; Sugár and Xu, 1992; Xu et al., 1994). The success rate of the VTF method in finding the global minimum can also be improved significantly by increasing the number of mixing times for the NOESY spectra, and by increasing the signal-to-noise ratio (Xu et al., 1994). In order to compare the STF and VARTIGO methods, all starting structures in Table 2 were also optimized using the STF given by Eq. 1. The R-factors for both the STF and VARTIGO optimizations are shown in Table 2. The final target function values are also listed for both methods. For the all-trans structure, the STF method resulted in R_m and R_d values of 0.46 and 0.169, respectively, suggesting that the optimization was trapped into a local minimum. In contrast, the VARTIGO method resulted in values of 0.39 and 0.08 for the same R-factors. Thus, the STF-optimized conformation deviates from the best GS structure while the VARTIGO method was able to find a structure very close to the best GS structure, as indicated by the R-factors in Table 2. In Fig. 4, we show a comparison of some of the interproton distances (corresponding to a subset of the experimental cross peaks) for the all-trans conformation before and after refinement by the STF and VARTIGO methods. The distances in the average VARTIGO structure were used as references (horizontal axis), and only distances up to 10 Å were included in the plots (some of the distances for the all-trans starting conformation exceed 20 Å). The better quality of the VARTIGO refinement is obvious from the figure. In a similar manner, for the M6 and M8 structures the VARTIGO method is able to avoid the local minima better than the STF method (e.g., compare all four R-factors). With the single exception of the M4 structure, where the STF method gave slightly better values for three of the R-factors (R_m, R_1 and R_2), the VARTIGO refinement gave R-factors which are generally better than or equally good as in the STF method. As mentioned above, in some specific instances,

such as the all-trans and the M8 structures, the improvement with VARTIGO is dramatic.

Ornithine side-chain orientation

Because of the twofold symmetry of the GS molecule, there was ambiguity in the assignment of some of the interresidue NOE contacts observed for the protons on the ornithine side chain. For example, the Orn-δNH_2 to Pro-αH cross peak could be between Orn[2] and either Pro[5] (as in NS) or Pro[10] (as in M1). The R-factor analysis failed to distinguish between these two choices. In the MEAN VARTIGO structure that we generated, the NOESY assignments corresponding to the M1 structure were assumed for the ornithine side chain. The principal difference between the M1 and NS structures is the orientation of the ornithine side chain. In the former, the Orn-δNH_2 group forms a hydrogen bond with Phe-CO in the i → i − 3 sense, while in the latter it forms a bond with Phe-CO in the i → i + 2 sense. This latter type of hydrogen bond was shown to be feasible in theoretical calculations (Némethy and Scheraga, 1984) and in experimental studies on GS in methanol (Krauss and Chan, 1982). Such a reorientation of the ornithine side chain is facilitated by large changes in the χ^1 and χ^2 torsion angles in the M1 (−63° and −170°) and NS (166° and 72°) conformations. Each type of orientation of GS predicts distinct types of NOE contacts, including intraresidue ornithine contacts (e.g., αH to βH_2 and γH_2). In our study, we found NOE contacts predicted for both types of orientation, suggesting that both conformations are present in DMSO with an exchange rate fast on the relaxation rate scale.

When the conformational exchange rate is much faster than the relaxation rates, the effective relaxation rate (or rate matrix) is a *weighted average* of relaxation rates (or rate matrices) for the individual conformations (Krishna et al., 1978,1980; Lee and Krishna, 1992; Moseley et al.,

1994a). When the conformational exchange rate is not very fast compared to the relaxation rates in macromolecular systems such as proteins and nucleic acids, one needs to employ a complete relaxation and conformational exchange matrix analysis in quantitating the NOESY spectra (Choe et al., 1991; Krishna and Lee, 1992; Lee and Krishna, 1992). An algorithm (CORCEMA) valid for an arbitrary number of states and arbitrary values of conformational exchange rates has been developed by our laboratory for analyzing NOESY spectra of such dynamical systems (Moseley et al., 1994a,b).

To simulate the NOESY contacts involving the ornithine side chain, we have defined an average relaxation rate matrix $<R>_{av}$ given by (Krishna et al., 1978, 1980; Lee and Krishna, 1992; Moseley et al., 1994a):

$$<R>_{av} = P_{M1} R_{M1} + P_{NS} R_{NS} \qquad (8)$$

where P_{M1} and P_{NS} ($= 1 - P_{M1}$) are fractional populations of the M1 and NS conformations, respectively. R_{M1} and R_{NS} correspond to the relaxation rate matrices for the M1 and Némethy–Scheraga structures, respectively. In principle, the populations could also serve as parameters to be optimized. The NOESY intensities were calculated using Eq. 9:

$$A(\tau_m) = \exp(-<R>_{av} \tau_m) A(0) \qquad (9)$$

where A is the matrix of intensities. In Fig. 5, we show experimental and backcalculated NOESY spectra for three different models: (1) M1; (2) NS; and (3) an equal mixture of M1 and NS conformations ($P_{M1} = 0.5$). The backcalculation for model (3) was done using Eqs. 8 and 9. It is easily seen that the third model approximates the experimental spectrum most closely. Thus, in DMSO the NOESY data on GS are compatible with the existence of two distinct conformations for the ornithine side chain,
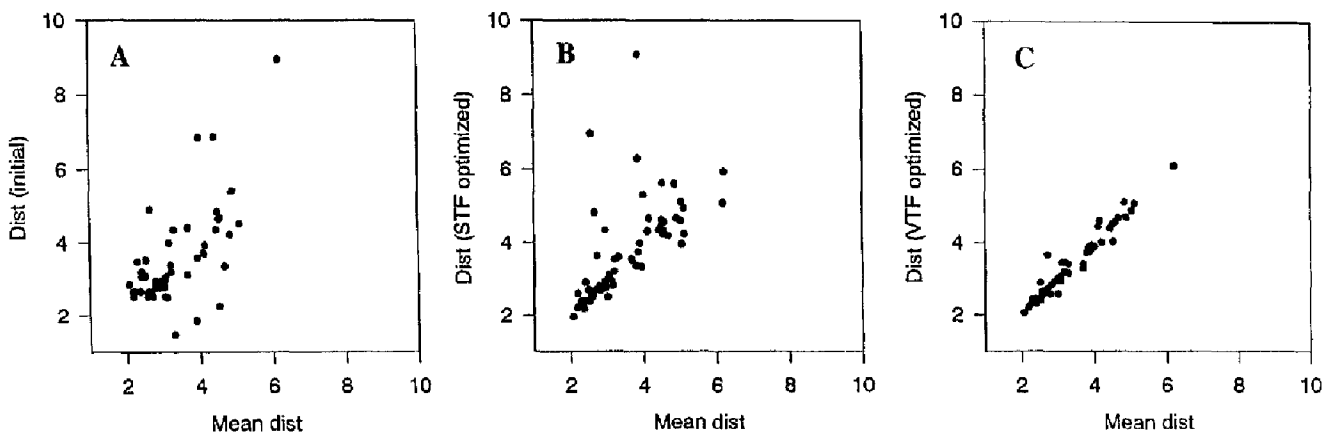

Fig. 4. Comparison of optimizations on the all-trans structure of gramicidin-S by the VARTIGO and STF methods. The points refer to a subset of experimental NOE contacts, since only distances less than 10 Å have been included in the plots. The average VARTIGO structure was used as the reference (horizontal axis). (A) Distances in the all-trans conformation prior to any optimization (some of the distances here are larger than 10 Å); (B) after refinement by the STF method; and (C) after refinement by the VARTIGO method.
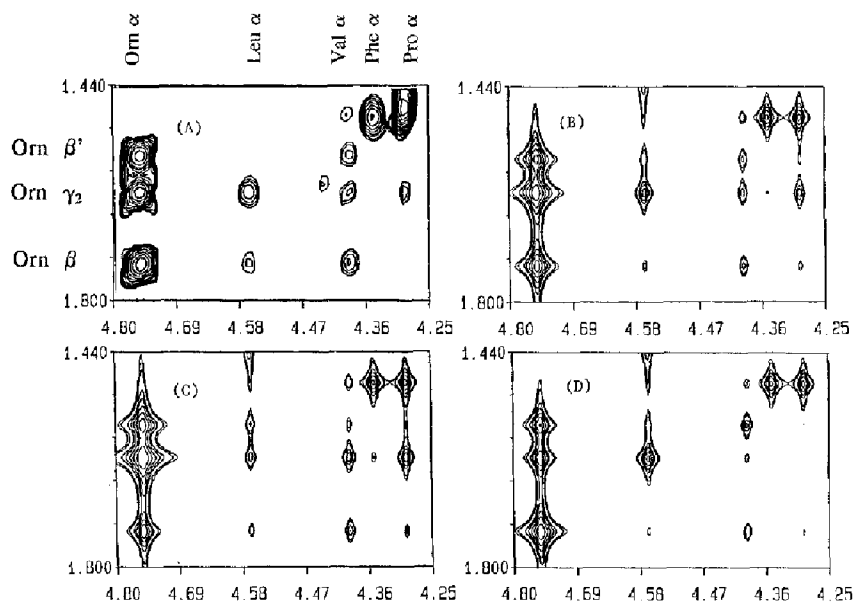
Fig. 5. Comparison of a portion of the experimental NOESY spectrum (containing ornithine intraresidue and some interresidue contacts) (A) with backcalculated spectra for three different models; (B) 50% each of the M1 and NS conformations (unoptimized) in fast exchange, calculated using Eqs. 8 and 9 in the text; (C) the unoptimized M1 model; and (D) the unoptimized NS model. Note the intraresidue NOE contacts between Orn-αH and its side-chain protons (β and γ).

corresponding to the M1 and NS structures, with an exchange rate fast on the relaxation rate scale. No attempt was made to optimize the individual M1 and NS side-chain orientations in this comparison, because currently the VARTIGO program can handle only one rigid molecule at a time. Such an optimization would have given an even better agreement between experimental and calculated spectra.

Conclusions

We have illustrated in this study the application of an intensity-refinement method for structure determination from experimental NOESY data. This method, called VARTIGO, employs a variable target function that is optimized using experimental intensities. Like most other methods, there are no guarantees that a global minimum will always be found with this method (e.g., the optimization of M9 that resulted in an optimized structure with a large R_1-factor). However, the success rate could be increased by (i) including as many widely different starting conformations (including all-trans) as possible; (ii) using NOESY data at several mixing times, including long mixing times where significant spin-diffusion effects will contribute to the intensities; and (iii) improving the signal-to-noise ratio (Xu et al., 1994). Optimization of the all-trans starting structure showed that the VTF optimization gives significantly better results than the single target function (STF) optimization. In this study, we have not made a comparison of the VARTIGO-based structures with those from an X-PLOR/QUANTA-based distance

geometry/simulated annealing calculation since, unlike ECEPP, the QUANTA program does not permit the generation of a linear peptide of gramicidin-S with an NH group at the N-terminus and a C=O at the C-terminus. A rigorous comparison of the VARTIGO- and X-PLOR-based calculations will be made in the near future on a linear polypeptide. Further, the current version of the VARTIGO algorithm does not incorporate an energy minimization step (other than assuming standard geometry, and energy minimization by ECEPP/3 of five structures to generate starting conformations for Table 2), whereas X-PLOR calculations involve a potential energy function in addition to the NOE constraint term.

This study also underscores the need to examine several different NOE R-factors *simultaneously* in judging the quality of an optimization. For example, for the M9(EM) optimized structure, the R_1 value (0.66) was not acceptable, even though the R_d value (≈ 0.11) appeared to be reasonable. On the other hand, the R_2 values for the VARTIGO and STF optimizations of the M3(EM) structure are identical, even though R_1 and R_m suggest that the VARTIGO method is better.

Finally, the NOESY data of GS in DMSO are compatible with the presence of two conformations for the ornithine side chain in fast exchange, one in which the Orn-$\delta NH_2 \rightarrow$ Phe-CO hydrogen bond is in the $i \rightarrow i + 2$ direction, and the other in the $i \rightarrow i - 3$ direction. The NOESY spectrum to represent this case was calculated using an average relaxation rate matrix (Eqs. 8 and 9) which is a weighted average of the relaxation rate matrices for the individual conformations.

48

Future developments in the refinement of VARTIGO will involve the inclusion of spectral density functions to handle complex internal motions (Sugár, 1992), the implementation of optimization routines to include conformational exchange (Lee and Krishna, 1992; Moseley et al., 1994a,b), and the implementation of efficient analytical gradient calculations in dihedral angle space (Abe et al., 1984; Mertz et al., 1991; Nesterova and Chuprina, 1993; Yip, 1993) to improve the efficiency of optimization for larger proteins. In the linear representation of gramicidin-S used in our analysis, the number of experimental constraints with a range k of 2 is 108, while the number with k > 2 is 14. As the protein size increases, the number of subsets with long-range constraints (k > 3) increases dramatically with the number of iterations. With more long-range constraints, the chances of overcoming local minima also improve for larger proteins. We hope to pursue refinements on larger proteins after the implementation of an efficient analytical gradient calculation in the VARTIGO procedure.

Acknowledgements

References

Abe, H., Braun, W., Noguti, T. and Gō, N. (1984) *Comput. Chem.*, 8, 239–247.

Bax, A. (1989) *Methods Enzymol.*, 176, 151–168.

Boelens, R., Koning, T.M.G. and Kaptein, R. (1988) *J. Mol. Struct.*, 173, 299–311.

Borgias, B.A. and James, T.L. (1988) *J. Magn. Reson.*, 79, 493–512.

Borgias, B.A. and James, T.L. (1989) *Methods Enzymol.*, 176, 169–183.

Borgias, B.A. and James, T.L. (1990) *J. Magn. Reson.*, 87, 475–487.

Braun, W. and Gō, N. (1985) *J. Mol. Biol.*, 186, 611–626.

Braun, W. (1987) *Q. Rev. Biophys.*, 19, 115–157.

Choe, B.Y., Cook, G. and Krishna, N.R. (1991) *J. Magn. Reson.*, 94, 387–393.

Crippen, G.M. and Havel, T.F. (1988) *Distance Geometry and Molecular Conformation*, Wiley, New York, NY.

Dennis, J.E., Gay, D.M. and Welsch, R.E. (1981) *ACM Trans. Math. Software*, 7, 369–383.

DeSantis, P. and Liquori, A.M. (1971) *Biopolymers*, 10, 699–710.

Dygert, M., Gō, N. and Scheraga, H. (1975) *Macromolecules*, 8, 750–761.

Ernst, R.R., Bodenhausen, G. and Wokaun, A. (1986) *Principles of Nuclear Magnetic Resonance in One and Two Dimensions*, Oxford University Press, New York, NY.

Esposito, G. and Pastore, A. (1988) *J. Magn. Reson.*, 76, 331–336.

Gondol, D. and Van Binst, G. (1986) *Biopolymers*, 25, 977–983.

Gonzalez, C., Rullmann, J.A.C., Bonvin, A.M.J.J., Boelens, R. and Kaptein, R. (1991) *J. Magn. Reson.*, 91, 659–664.

Güntert, P., Braun, W. and Wüthrich, K. (1991) *J. Mol. Biol.*, 217, 517–530.

Huang, D.H., Walter, R., Glickson, J.D. and Krishna, N.R. (1981) *Proc. Natl. Acad. Sci. USA*, 78, 672–675.

Hull, S.E., Karlsson, R., Woolfon, M.M. and Hull, E.J. (1978) *Nature*, 275, 206–207.

Jones, C.R., Sikakana, C.T., Hehir, S., Kuo, M.C. and Gibbons, W.A. (1978) *Biophys. J.*, 24, 815–832.

Keepers, J.W. and James, T.L. (1984) *J. Magn. Reson.*, 57, 404–426.

Koning, T.M.G., Boelens, R. and Kaptein, R. (1990) *J. Magn. Reson.*, 90, 111–123.

Krauss, E.M. and Chan, S.I. (1982) *J. Am. Chem. Soc.*, 104, 6953–6961.

Krishna, N.R., Agresti, D.G., Glickson, J.D. and Walter, R. (1978) *Biophys. J.*, 24, 791–814.

Krishna, N.R., Goldstein, G. and Glickson, J.D. (1980) *Biopolymers*, 19, 2003–2021.

Krishna, N.R. and Lee, W. (1992) *Biophys. J.*, 61, A33.

Kuntz, I.D., Thomason, J.I. and Oshiro, C.M. (1989) *Methods Enzymol.*, 177, 159–203.

Lee, W. and Krishna, N.R. (1992) *J. Magn. Reson.*, 98, 36–48.

Macura, S. and Ernst, R.R. (1980) *Mol. Phys.*, 41, 95–117.

Mertz, J.E., Güntert, P., Wüthrich, K. and Braun, W. (1991) *J. Biomol. NMR*, 1, 257–269.

Mirau, P.A. (1988) *J. Magn. Reson.*, 80, 439–447.

Moseley, H.N.B., Curto, E.V. and Krishna, N.R. (1994a) *J. Magn. Reson.*, submitted for publication.

Moseley, H.N.B., Curto, E.V. and Krishna, N.R. (1994b) Abstract #WP115, 35th Experimental NMR Conference, Asilomar, CA.

Némethy, G. and Scheraga, H.A. (1984) *Biochem. Biophys. Res. Commun.*, 118, 643–647.

Nesterova, E.N. and Chuprina, V.P. (1993) *J. Magn. Reson. Ser. B*, 101, 94–96.

Niccolai, N., Rossi, C., Mascagni, P., Neri, P. and Gibbons, W. (1984) *Biochem. Biophys. Res. Commun.*, 124, 739–744.

Nilges, M. (1993) *Proteins*, 17, 297–309.

Otting, G., Widmer, H., Wagner, G. and Wüthrich, K. (1986) *J. Magn. Reson.*, 66, 187–193.

Post, C.B., Meadows, R.P. and Gorenstein, D.G. (1990) *J. Am. Chem. Soc.*, 112, 6796–6803.

Rae, I.D., Stimson, E.R. and Scheraga, H.A. (1977) *Biochem. Biophys. Res. Commun.*, 77, 225–229.

Rance, M., Sørensen, O.W., Bodenhausen, G., Wagner, G., Ernst, R.R. and Wüthrich, K. (1983) *Biochem. Biophys. Res. Commun.*, 117, 479–485.

Sugár, I.P. (1992) *J. Phys. Chem.*, 96, 10719–10724.

Sugár, I.P. and Xu, Y. (1992) *Prog. Biophys. Mol. Biol.*, 58, 61–84.

Thomas, P.D., Basus, V.J. and James, T.L. (1991) *Proc. Natl. Acad. Sci. USA*, 88, 1237–1241.

Woessner, D.E. (1962) *J. Chem. Phys.*, 36, 1–4.

Wüthrich, K. (1986) *NMR of Proteins and Nucleic Acids*, Wiley, New York, NY.

Xu, Y. and Sugár, I.P. (1993) *J. Magn. Reson. Ser. B*, 101, 145–157.

Xu, Y., Krishna, N.R. and Sugár, I.P. (1995) *J. Magn. Reson.*, in press.

Yip, P.F. (1993) *J. Biomol. NMR*, 3, 361–365.